Conformational Heterogeneity Is Revealed in the Dissociation of the Oligomeric Chaperonin GroEL by High Hydrostatic Pressure†

Markandeswar Panda and Paul M. Horowitz*

Department of Biochemistry, Mail Code 7760, University of Texas Health Science Center at San Antonio, 7703 Floyd Curl Drive, San Antonio, Texas 78229-3900

Received September 14, 2001; Revised Manuscript Received December 5, 2001

ABSTRACT: We investigated the dissociation of tetradecameric GroEL by high hydrostatic pressure in the range of 1−2.5 kbar. Kinetics of the dissociation of GroEL in the absence and presence of Mg^{2+} and/or KCl were monitored using light scattering. All of the kinetics were biphasic in nature. At any given pressure, only monomers and 14mers were produced, and below 2.5 kbar, the 14mers only partially dissociated to monomers, which did not significantly reassemble on depressurization. Under identical reaction conditions, the observed dissociation rates decreased by only 2-fold when the concentration of GroEL was increased by 20-fold. At 2.5 kbar the observed rates decreased exponentially with the increase in [KCl] and reached a minimum at ∼75 mM. Similarly, the rates decreased with the increase in [Mg^{2+}] and reached a minimum at ∼3 mM Mg^{2+}. In the presence of saturating amounts of Mg^{2+} (10 mM) and KCl (100 mM), the rates were much faster than with 10 mM Mg^{2+} alone. The results could be rationalized in terms of the presence of GroEL heterogeneity, which could not be assessed easily by common techniques such as sedimentation velocity, HPLC, gel electrophoresis, and dissociation by chaotropes**.** This heterogeneity is evidence of subpopulations of GroEL that dissociate at different pressures. At low pressures, the oligomer without added Mg^{2+} only partially dissociates to monomers, leading to an apparent plateau in the kinetics, whereas in the presence of Mg^{2+} the species are converted to a tighter Mg^{2+}-bound species, leading to a much slower dissociation process. The presence of KCl in the sample also leads to similar heterogeneity.

High hydrostatic pressure techniques are becoming important tools in studying dissociation of oligomeric proteins, protein aggregates, and unfolding of monomeric proteins (*1*−*11*) in the absence of externally added chaotropes. The use of high-pressure studies provides new insights into protein folding, protein misfolding, aggregation, protein−protein interactions, and virus assembly (*12*). The important theories behind this technique and excellent experimental details can be found in several edited books and monographs (*1*, *13*−*18*). In a recent publication, we have briefly summarized the physical forces responsible for the dissociation of oligomers by high hydrostatic pressure (*19*). Although pressures above 3−4 kbar[1] can denature many proteins (*1*, *20*, *21*), at pressures below 3 kbar, oligomeric proteins or protein assemblies generally undergo reversible dissociation into subunits (*5*, *21*). It has been observed that the resulting monomers may undergo conformational drifts away from their conformations in the oligomer and, therefore, may not reassociate rapidly upon depressurization (*19*, *22*).

Dissociation of a number of oligomeric proteins by high hydrostatic pressure has been studied. Studies on dimers (*5*, *6*, *11*, *20*, *23*−*27*), trimers (*28*), tetramers (*25*, *29*−*32*), and higher order aggregates (*2*, *3*, *21*, *33*−*37*) have provided interesting information on the equilibria between the oligomer and the resulting monomers. Such studies have led to the understanding of the transition from stochastic to deterministic equilibria in the dissociation processes of oligomeric proteins (*1*, *5*, *25*). The dynamic equilibrium between oligomers and dissociated monomers where all species rapidly interconvert on the time scale of measurement, known as stochastic equilibrium, has been shown to be fully applicable only to very simple dimeric proteins (*38*, *39*). However, significant departures from this simple thermodynamic equilibrium have been reported due to heterogeneity in the samples and slow conformational drifts in the dissociated monomers (*1*, *26*, *35*, *40*, *41*). It has been reported that the pressure-induced dissociation of erythrocruorin from the oligochete worm *Glossoscolex paulistus* (MW = 3.1×10^6, 12 octameric subunits with a total of 96 monomer subunits) (*42*), the capsid of the Brome Mosaic virus (*33*), and hemocyanin (*43*) shows only small dependence on concentration. This led to the conclusion that these oligomers contain heterogeneous populations of forms, each having its own characteristic dissociation pressure, which is defined as the deterministic dissociation (*1*, *5*, *25*). In a recent publication, Ferreira and Felice (*44*) have drawn many important conclusions from the study of deterministic behavior of proteins and their implications in understanding conformational diseases.

† This research was supported by National Institutes of Health Grant NIHGM25177 and Robert A. Welch Foundation Grant AQ723 (to P.M.H.).

* To whom communication should be addressed. Telephone: (210) 567-3737. Fax: (210) 567-6595. E-mail: horowitz@biochem.uthscsa.edu.

[1] Units of pressure: 1 bar = 0.1 MPa (megapascal) = 0.987 atm = 14.5 psi (pounds/in.^{2}); 1 kbar = 1000 bar. Abbreviation: DTT, dithiothreitol (*threo*-1,4-dimercapto-2,3-butanediol).

10.1021/bi011794c CCC: $22.00
Published on Web 01/15/2002

The bacterial chaperonin GroEL is an excellent model for studying the effect of high hydrostatic pressure on the dissociation of macromolecular assemblies. GroEL and its cochaperonin GroES are multimeric proteins that assist folding of other proteins by preventing misfolding and aggregation. Mutational studies have demonstrated that both chaperonins are essential for protein folding *in vivo* (*45*−*47*). GroEL is a tetradecamer (14mer) of 57 kDa subunits arranged in two, seven-membered rings stacked back to back to yield a cylindrical structure. There are no tryptophan residues, and each subunit contains three cysteines: Cys138, Cys458, and Cys519. The X-ray crystal structures of GroEL (*48*, *49*), GroEL fully complexed with 14 ATPγS molecules (*50*), and the GroEL−GroES−$(ADP)_7$ complex (*51*) are available. The crystal structure demonstrates that each monomer is folded into three distinct domains. First, the apical domain faces the solvent and forms the opening to the central channel and contains the peptide-binding site; second, a highly helical equatorial domain is the ATP-binding site and forms the inter- and intra-ring contacts; and third, a hinge-like intermediate domain links the apical and equatorial domains. The GroEL-assisted protein folding reaction cycle consists of a number of sequential reactions such as the binding of the polypeptide at the apical domains of the cis ring, binding of seven molecules of ATP and GroES, forming a stable cis assembly, and freeing the tightly bound polypeptide into a protected, enclosed space where it folds with hydrolysis of ATP. Further steps lead to release of ADP, GroES, and the folded polypeptide (*51*−*54*). In addition to GroES and ATP, the presence of Mg^{2+} and K^+ is also necessary for the GroEL-assisted folding (*55*−*59*). The role of ATP is important both as an energy source and as an allosteric effector. ATP binding displays both intra-ring positive cooperativity and inter-ring negative cooperativity (*60*, *61*). The binding of ATP has been suggested to destabilize the quaternary structure of GroEL (*62*). Although other divalent cations such as Ca^{2+} are known to stabilize macromolecular assemblies (*63*, *64*), the role of Mg^{2+} as a structural ligand is important for the GroEL−GroES system (*55*−*59*).

In an earlier investigation, we reported that high hydrostatic pressure can dissociate GroEL tetradecamers (*65*). After depressurization, the monomers reassociated back to the oligomer only very slowly with a $t_{1/2}$ of 150 h at 25 °C. The dissociation and association reactions were facilitated by MgATP only if it was present during pressurization. From their reassociation properties, it has been demonstrated that the monomers formed by pressure dissociation of the 14mer are different from those formed by the action of 2.5 M urea (*65*). Recently, we have reported some effects of high hydrostatic pressure on GroEL, GroES, and the GroEL−GroES−$(ADP)_7$ complex in the absence and presence of Mg^{2+} and adenine nucleotides (*19*). Although there has been no direct evidence for the presence of conformational heterogeneity in the purified GroEL samples, the results from the present investigation suggest its presence. During the isolation and purification of GroEL several reagents such as Mg^{2+} and KCl are added, and it is possible that such binding might produce heterogeneous populations of GroEL bound by these reagents. Recently, using atomic force microscopy (AFM) studies Vinckier et al. (*66*) have detected the presence of heterogeneity in the interactions between GroEL and substrate proteins. Although Thirumalai and Lorimer (*54*) attribute this heterogeneity to the substrate protein, it is very possible that part of such heterogeneity exists in GroEL itself. In the present investigation, we present evidence that the dissociation equilibrium is deterministic along with the evidence for heterogeneity in the GroEL 14mer.

MATERIALS AND METHODS

GroEL was purified from lysates of *Escherichia coli* cells bearing the multicopy plasmid pND5 using a modified version of a previously described procedure (*67*). Details of the modifications can be found in an earlier publication (*68*). The fluorescent contaminants from the isolated GroEL were removed by eluting the protein from a Reactive Red 120 agarose (type 3000-CL) column equilibrated with a 50 mM Tris-HCl buffer, pH 7.5, 5 mM Mg^{2+}, and 0.5 mM DTT at 4 °C (*69*). The final preparation gave single bands by both native and denaturing gel electrophoresis. The buffer solutions used in the kinetics experiments were filtered through 0.2 μm surfactant-free cellulose acetate membrane syringe filters (Nalgene). Tris buffer is suitable for pressure experiments because of the small pK_a dependence upon hydrostatic pressure (*70*).

High-Pressure Experiments. The high-pressure cell and photon counting spectrofluorometer were from ISS Inc., Champaign, IL. The ISS K2 multifrequency phase fluorometer is equipped with water-cooled PMT housing. In the photon counting mode, the responses are linear up to 4.0×10^6 counts per second (cps). In the present investigation, in most of the experiments the photon counts were kept below 1.0×10^6 cps although in some experiments it was $\sim 1.6 \times 10^6$ cps. The stainless steel alloy cell with quartz windows can be pressurized up to 3 kbar. Protein samples for the experiments were contained in quartz bottles (1 mL volume) with pressure caps (provided by ISS). Spectroscopic grade ethanol was used as the pressurizing fluid. The high-pressure generator was from Advanced Pressure Products (APP), Ithaca, NY. The pressure generator is electronically controlled and programmable to obtain pressure gradients. The temperature of the high-pressure cell was maintained by a circulating water bath. Two independent computers controlled the APP pressure generator and ISS spectrofluorometer. The target pressure was controlled by computer using a program written for the APP software. The generated data were imported to Origin software (Version 6; Microcal Software, Northampton, MA) and analyzed. Kinetics experiments were done by first equilibrating the protein sample in the pressure cell for 1 h at the desired temperature. After equilibration, the fluorometer recording was turned on, followed by the pressure machine. GroEL dissociation was followed by monitoring light scattering at 400 nm. The excitation and emission slits were 2 mm (16 nm band-pass) and 1 mm (8 nm band-pass), respectively. In typical experiments, to reach pressures of 1 kbar required 1 min, 2 kbar required 3 min, and 2.5 kbar required 4.5 min at a pump speed of 2.0. The limitations and reasons to avoid fast pressurization and depressurization have been discussed in our earlier work (*19*). In general, rapid pressure changes cause damage by shattering the quartz windows or sample bottles. Control experiments using latex beads have shown that the intensity changes were not contributed by dimension changes of the cell due to high pressure (*19*).

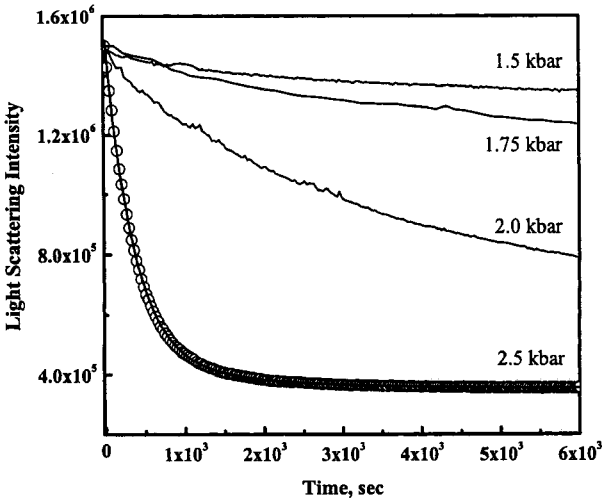

FIGURE 1: Effect of pressure on the kinetics of dissociation of the GroEL 14mer. GroEL was dissociated at definite pressures as described in Materials and Methods, and kinetics were monitored using scattering at 400 nm (excitation and emission) until the reactions reached plateaus. For the sake of clarity only parts of kinetics at 1.5, 1.75, and 2.0 kbar are shown in the figure. The kinetics at 2.5 kbar represents a typical plot of data, light scattering intensity (cps) versus time in seconds. The solid line through the data (open circles) is a fit to the data using a biexponential equation (see Materials and Methods). The plateau values obtained from biexponential fits (see Materials and Methods) of the data were 1.34×10^6, 8.22×10^5, 4.30×10^5, and 3.55×10^5 cps at 1.5, 1.75, 2.0, and 2.5 kbar, respectively (see Results). Taking the reaction at 2.5 kbar, where the monomer formation was complete as 100%, the apparent extent of reactions at 1.5, 1.75, and 2.0 kbar correspond to ~14%, 59%, and 93%, respectively (see Results). The reaction conditions were $[\text{GroEL}]_{14\text{mer}} = 0.36$ μM, Tris = 50 mM, pH = 7.8, and $T = 25$ °C. Other conditions for monitoring the kinetics and pressure setup are in Materials and Methods.

Analysis of Kinetic Data. The data were truncated to take account of the time taken by the pressure cell to reach the target pressure. The rates were evaluated by fitting the data to either mono- or biexponential equations: $Y = A_1 \exp(-k_1 t) + A_2$ or $Y = A_1 \exp(-k_1 t) + A_2 \exp(-k_2 t) + A_3$, respectively. The independent variable Y was the observed scattering intensity in counts per second (cps) after subtracting the scattering due to buffer. The pseudo-first-order rate constants k_1 and k_2 and the parameters relating the amplitudes A_1, A_2, and A_3 were obtained from iterative nonlinear least-squares regression of the data using the Origin software program (MicroCal). To confirm that the kinetics profiles are free from artifacts due to photon pileup, we repeated some of the experiments at photon counts at ~250000 cps. We did not observe any changes in the observed rates from the same experiment done at the two different intensities. Additionally, the analysis of any part of a specific kinetic trace resulted in identical parameters for that experiment.

RESULTS

Kinetics of the dissociation of the GroEL14mer at pressures 1.5, 1.75, 2.0, and 2.5 kbar were studied for about 10 half-lives at 25 °C in 50 mM Tris-HCl buffer, pH = 7.8. Typical kinetics followed by light scattering and their biexponential fits at 2.5 kbar are shown in Figure 1. In this figure, parts of kinetics traces at 1.5, 1.75, and 2.0 kbar are included to show that the dissociation process becomes faster at increasing pressures and proceeds to more dissociated monomers (plateau or infinity values). The plateau values obtained from biexponential fits (see Materials and Methods) of the data were 1.34×10^6, 8.22×10^5, 4.30×10^5, and 3.55×10^5 cps at 1.5, 1.75, 2.0, and 2.5 kbar, respectively. Formation of increasing amounts of monomers with increase in the applied pressure has been confirmed from the analysis of products by native gel electrophoresis after reactions reached apparent plateaus in the kinetics at various pressures (*19*). In this study, considering the infinity value of 3.55×10^5 cps (see Figure 1), where monomer formation is complete (100%), the apparent extent of reactions at 1.5, 1.75, and 2.00 kbar correspond to ~14%, 59%, and 93%, respectively, of the reaction at 2.5 kbar. It is interesting to note that the dissociation kinetics at 2.5 kbar in 50 mM Tris buffer shown in Figure 1 was fit to biexponential kinetics with $k_{1,\text{obs}} = 2.86 \pm 0.02) \times 10^{-3}$ s^{-1} and $k_{2,\text{obs}} = (7.00 \pm 0.30) \times 10^{-4}$ s^{-1}, whereas in the earlier study it was clearly a monoexponential with $k_{\text{obs}} = (4.00 \pm 0.04) \times 10^{-3}$ s^{-1}. Here, the amplitude of the fast phase was about 90% of the total amplitude obtained from the biexponential fit. Since the reaction temperature in this study was 25 °C instead of 20 °C that was used in the earlier investigation (*19*), a rate faster than 4.00×10^{-3} s^{-1} was expected. To avoid the high stress on the quartz windows, the reaction temperature for this investigation was maintained at 25 °C to make the reactions slightly faster for studying the extremely slow reactions under high hydrostatic pressure.

Figure 2 represents a series of pressurization−depressurization−repressurization sequences on a sample of GroEL in the absence of any added ligand in 50 mM Tris, pH = 7.8, $T = 25$ °C. Panel A shows the typical biphasic kinetics at 1.75 kbar. After the reaction approached its plateau value, it was depressurized to 1 bar and then repressurized back to 1.75 kbar (Figure 2, panel B). The purpose of this experiment was to determine whether the depressurized monomers reassemble and could be dissociated at the same (1.75 kbar) pressure. It was observed that such pressurization does not lead to any significant decrease in the light scattering intensity (Figure 2, panel B). Although the data shown are a reapplication of pressure after only ~17 min, we have done another experiment where the sample was equilibrated at 1 bar for 24 h, which again does not significantly reassemble nor does it lead to further detectable dissociation upon raising the pressure to 1.75 kbar. Thus under these conditions of time and pressure, this represents an apparently stable distribution. Fitting the data (Figure 2, panel B) to a monoexponential equation (see Materials and Methods) produced an observed rate (1.2×10^{-4} s^{-1}) that is very similar in magnitude to the slow phase of the biexponential fit of the main reaction at 1.75 kbar ($k_{2,\text{obs}} = 1.5 \times 10^{-4}$ s^{-1}), which is shown in Figure 2, panel A. This leads to the conclusion that at 1.75 kbar the kinetics reached completion and only a small fraction of a species that dissociated at this pressure reassociated upon depressurization. This small fraction of reassociated species led to the slow kinetics (Figure 2, panel B) upon repressurization to 1.75 kbar. We did similar experiments in which the sample was pressurized to 2.0 kbar and then depressurized to 1 bar and finally repressurized to 2 kbar. Similarly, we cycled samples between 1.5 kbar and 1 bar. In each case, we observed similar trends in the kinetics. To demonstrate that the fraction remaining at each pressure could dissociate at higher

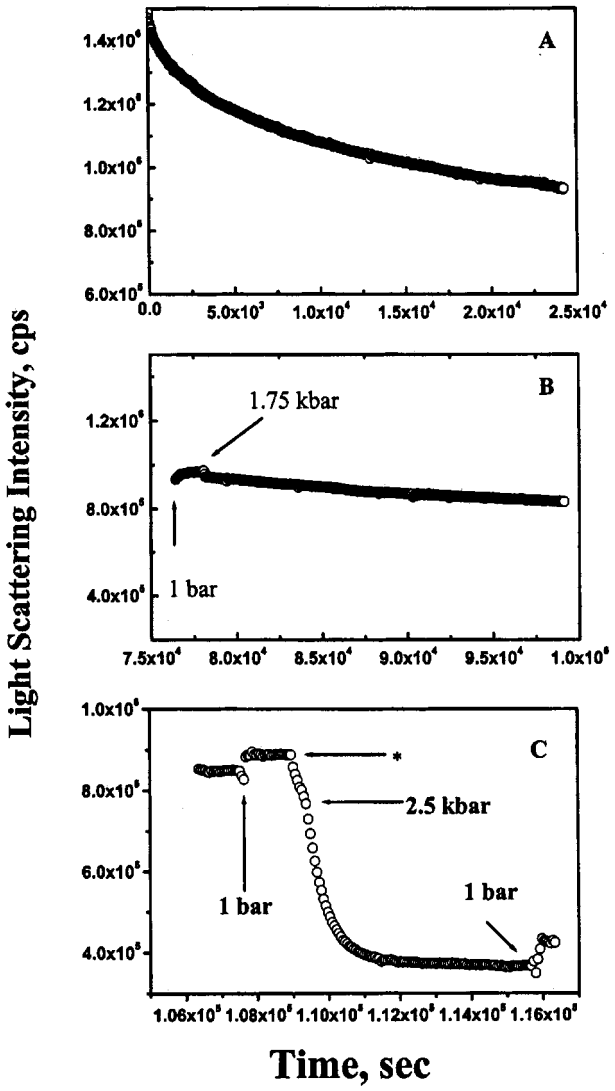

FIGURE 2: Effect of repressurization to 1.75 kbar and then to 2.5 kbar pressure on the remaining GroEL 14mer after initial dissociation of a 14mer species at 1.75 kbar. Dissociation kinetics was followed as described in Materials and Methods. The reaction conditions were $[GroEL]_{14mer} = 0.36$ μM, Tris = 50 mM, pH = 7.8, and $T = 25$ °C. All of the reactions shown in the three panels (A, B, and C) are using the same sample of GroEL in the pressure cuvette and under identical setup of the instrument parameters except for the applied pressures as discussed. All of the times presented on the abscissa of the panels are continuous with the initial zero at the beginning of panel A. The reaction was monitored for 6 h 45 min at 1.75 kbar, which followed biexponential kinetics (panel A). It was continued until 21 h 15 min until it appeared to reach a plateau and depressurizd to 1 bar (data not shown). The recording of the data after this time is shown in panel B. After ~25 min the sample was repressurized to 1. 75 kbar and monitored for another 6 h 15 min (panel B). Panel C: The reaction sample was depressurized again to 1 bar after a plateau was reached (29 h 50 min) and pressurized to 2.5 kbar (at 30 h 15 min, denoted by an asterisk in panel C). The time at which the pressure reached 2.5 kbar is denoted by a horizontal arrow. The kinetics at this pressure are identical in rates (biexponential) to those observed using a nonpressurized sample of GroEL (see Figure 1, kinetics at 2.5 kbar).

pressure, the sample at the completion of the kinetics shown in Figure 2, panel B, for example, was depressurized to 1 bar after the reaction reached a plateau followed by pressurization to 2.5 kbar. The kinetic plot is shown in Figure 2, panel C. It is very clear that the large fraction of GroEL 14mers that remained undissociated at 1.75 kbar could be completely dissociated to monomers by increasing the pressure to 2.5 kbar. The data for the reaction after 2.5 kbar pressure was reached were fit to a monoexponential equation (see Materials and Methods) and produced a k_{obs} value of $(1.9 \pm 0.1) \times 10^{-3}$ s^{-1}. Although this value is not identical in magnitude to the observed fast rate, $k_{1,obs} = [(2.86 \pm 0.02) \times 10^{-3}$ s$^{-1}]$ from a separate experiment done at this pressure of 2.5 kbar (see trace corresponding to 2.5 kbar in Figure 1), the kinetics confirm that the remaining species which did not dissociate at 1.75 kbar are responsible for the process seen at 2.5 kbar in panel C. The lower value of the observed rate in the repressurization experiment in Figure 2, panel C, compared with the direct pressurization experiment (Figure 1 and Table 1). The infinity value of this reaction also reached the same value seen in Figure 1. In our earlier work we had concluded that the dissociation at any given pressure is governed by both kinetics and equilibria of a heterogeneous population of GroEL (*19*). The present results provide direct evidence for this.

Table 1: Effect of KCl and Mg^{2+} on the Observed Dissociation Rates of GroEL at 2.5 kbar[a]

reagent	$k_{1,obs}$, s^{-1}	$k_{2,obs}$, s^{-1}
buffer only	$(2.86 \pm 0.02) \times 10^{-3}$ (91)[b]	$(7.00 \pm 0.30) \times 10^{-4}$ (9)[b]
10 mM Mg^{2+}	$(1.20 \pm 0.02) \times 10^{-4}$ (24)[b]	$(1.00 \pm 0.08) \times 10^{-5}$ (76)[b]
100 mM KCl	$(6.40 \pm 0.20) \times 10^{-4}$ (20)[b]	$(9.00 \pm 0.10) \times 10^{-5}$ (80)[b]
10 mM Mg^{2+} + 100 mM KCl	$(1.50 \pm 0.07) \times 10^{-4}$ (19)[b]	$(2.00 \pm 0.06) \times 10^{-5}$ (81)[b]

[a] Conditions: $[GroEL]_{14mer} = 0.36$ μM, Tris = 50 mM, pH = 7.8, and $T = 25$ °C. [b] The values in parentheses in percent are the relative amplitudes of the corresponding phase of the observed biphasic kinetics. The amplitudes for phases corresponding to the observed rates $k_{1,obs}$ and $k_{2,obs}$ refer to A_1 and A_2, respectively, in the biexponential equation (see Materials and Methods). The total amplitude of the reaction is taken as 100%.

In our earlier investigation, we speculated that the monomers formed in the pressure dissociation undergo conformational drift and therefore do not readily reassociate (*19*). Since there are three cysteines in each monomer of the GroEL, one might suspect that the irreversibility of the dissociation process even after 24 h of depressurization could be attributed to disulfide formation. This could be due to both inter- and intramolecular disulfide formation from thiol oxidation and other chemical modification. To test this, we did a dissociation experiment at 2.5 kbar with the GroEL 14mer in a buffer containing 1 mM EDTA and 5.0 mM DTT (dithiothreitol) to avoid thiol oxidation. The dissociated monomers did not show any increase in intensity even after 24 h after depressurization to 1 bar. Therefore, in the present investigation, thiol oxidation as the cause of irreversibility can be ruled out.

The effect of GroEL 14mer concentration on the dissociation kinetics at 2.5 kbar in buffer without Mg^{2+} or KCl was studied under identical experimental conditions (see Materials and Methods) by varying the concentration of the protein from 0.09 to 1.8 μM (20-fold). The results are shown in Figure 3. The data were fit to a straight line (solid line in the figure), which yielded a slope of $(-7.2 \pm 2.1) \times 10^{-4}$ s^{-1} μM^{-1} and an intercept of $(2.6 \pm 0.2) \times 10^{-3}$ s^{-1}. Therefore, the observed rates decreased only about 2-fold when the concentration of the protein was varied 20-fold and can be considered to be independent of the $[GroEL]_{14mer}$ in the range investigated. This slight reduction in the

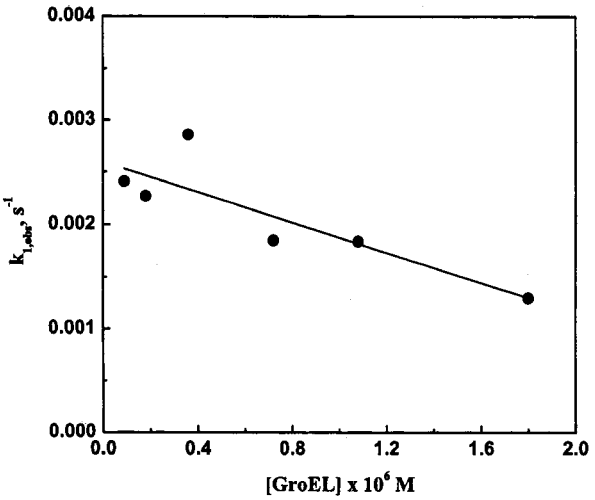

FIGURE 3: Effect of GroEL concentration on the observed dissociation rate at 2.5 kbar. Only the plot of $k_{1,obs}$ vs $[GroEL]_{14mer}$ is shown. This faster phase has about 70% of the total amplitude of the dissociation reaction. The slower phase ($k_{2,obs}$) at any specific concentration of GroEL was about 12−15 times slower than the corresponding fast phase and showed independence on $[GroEL]_{14mer}$ (see Results). The reaction conditions were Tris = 50 mM, pH = 7.8, and T = 25 °C. Other conditions for monitoring the kinetics and pressure setup are in Materials and Methods.

observed rate could be related to the some unknown association of the 14mers as the concentration becomes sufficiently high. However, there is no other proof for such association from the results from this investigation, and such proof is beyond the scope of this investigation. This independence of dissociation on the concentration of proteins or aggregates have been designated as a state of "deterministic equilibrium" (*1*, *25*, *71*, *72*) and has been observed for hemocyanin (*43*), erythrocruorin (*42*), and the capsid of Brome Mosaic virus (*33*).

Since KCl and Mg^{2+} are also used in the purification of GroEL, we studied their effects to determine whether their presence is related to the observed heterogeneity. As stated in the introduction, in addition to GroES and ATP, the ions K^+ and Mg^{2+} are also necessary for the GroEL-assisted protein folding (*55*−*59*). Plots of the fast ($k_{1,obs}$) and slow ($k_{2,obs}$) observed rates from the biphasic kinetics versus the concentration of KCl (0−100 mM) are shown in Figure 4, panels A and B, respectively. In both cases, the rates decrease exponentially as the concentration of KCl is increased and reach a plateau at ∼75 mM KCl. This is a clear indication that KCl imparts some tightness to the GroEL 14mer by the formation of salt bridges that are broken in a kinetically controlled process leading to slower observed dissociation rates. The identical exponential decrease observed in both $k_{1,obs}$ and $k_{2,obs}$ values with increasing KCl most probably points out the presence of at least two kinds of species present in the GroEL preparation.

The effects of added Mg^{2+} on the fast ($k_{1,obs}$) and slow ($k_{2,obs}$) phases of the biphasic rates are shown in Figure 5, panels A and B, respectively. Both of the observed rates decrease exponentially as the concentration of Mg^{2+} increased. In this regard it is interesting to compare the dissociation of GroEL at 2.5 kbar in the presence of 10 mM Mg^{2+} (saturating amount as seen from Figure 5) from two different preparations. In the earlier study at 20 °C the biphasic kinetics yield $k_{1,obs}$ and $k_{2,obs}$ values of 5.0×10^{-3}

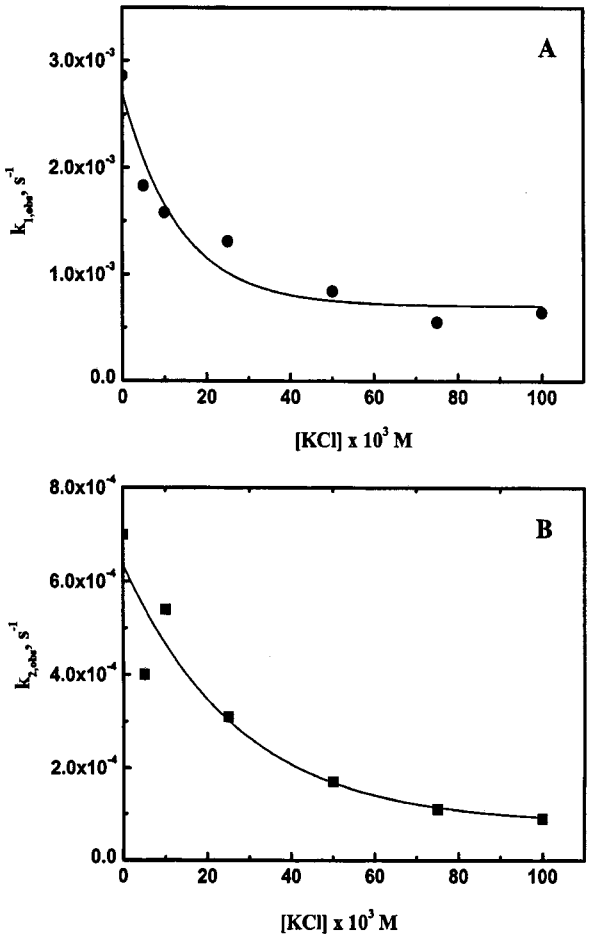

FIGURE 4: Effect of added KCl on the dissociation rate of GroEL at 2.5 kbar. The observed fast ($k_{1,obs}$, solid circles) and slow ($k_{2,obs}$, solid squares) rates obtained from biexponential fits versus [KCl] are shown in panels A and B, respectively. The lines drawn through the data are only for the purpose of visualizing the data. The reaction conditions were $[GroEL]_{14mer}$ = 0.36 μM, Tris = 50 mM, pH = 7.8, and T = 25 °C.

s^{-1} (∼5% of total amplitude) and 8.0×10^{-5} s^{-1} (∼95% of total amplitude), respectively (*19*). In the present study at 25 °C, we expected higher magnitudes of the observed rates, but the values are found to be $k_{1,obs} = 1.2 \times 10^{-4}$ (∼24% of total amplitude) and $k_{2,obs} = 1.0 \times 10^{-5}$ s^{-1} (∼76% of total amplitude). Since these two preparations behave identically on native gel electrophoresis, the most reasonable explanation is that the small amounts of Mg^{2+} bound to GroEL do not produce detectable mobility changes. From mutational studies on the single ring (SR1) and double ring GroEL, Rye et al. (*73*) have shown that the carboxylate group of aspartate at position 398 directly coordinates with Mg^{2+} and exhibits only ∼2% ATP hydrolysis activity. Therefore, we conclude that the presence of heterogeneous GroEL species formed by binding different amounts of this metal ion is very probable in most of the preparations. The presence of such species could lead to the deterministic behavior exhibited by GroEL in the high-pressure dissociation experiments.

To understand the combined effect of added Mg^{2+} and KCl on the dissociation rates at a pressure of 2.5 kbar, experiments were done at 10 mM Mg^{2+} and 100 mM KCl where the kinetics reach their minimum values. The results are summarized in Table 1. The $k_{1,obs}$ (fast) rates are in the order buffer only > 100 mM KCl > 10 mM Mg^{2+}+100

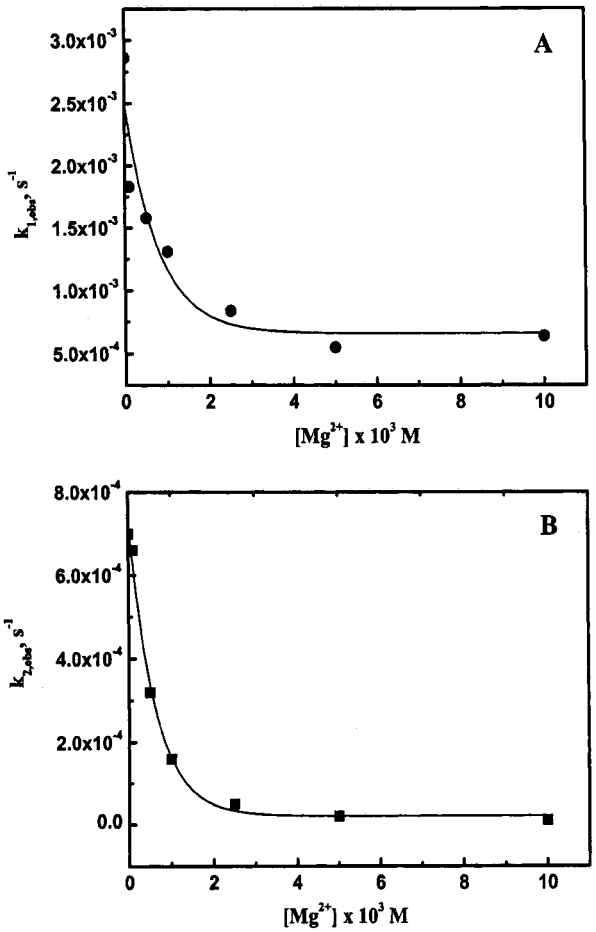

FIGURE 5: Effect of added $MgCl_2$ on the dissociation rate of GroEL at 2.5 kbar. The observed fast ($k_{1,obs}$, solid circles) and slow ($k_{2,obs}$, solid squares) rates obtained from biexponential fits versus [Mg^{2+}] are shown in panels A and B, respectively. The lines drawn through the data are only for the purpose of visualizing the data. The reaction conditions were $[GroEL]_{14mer} = 0.36$ μM, Tris = 50 mM, pH = 7.8, and $T = 25$ °C.

mM KCl > 10 mM Mg^{2+}; the $k_{2,obs}$ (slow) rates are in the order buffer only > 100 mM KCl > 10 mM Mg^{2+}+ 100 mM KCl > 10 mM Mg^{2+}. It is interesting to note that, in the fast phase in the buffer alone, the dissociation has the maximum amplitude (91% total), whereas the slow phase of the reactions in the presence of Mg^{2+}, KCl, and Mg^{2+} + KCl has the maximum amplitude. This observation appears as a change in the dissociation mechanism at this constant pressure of 2.5 kbar, most probably due to the change in the ratios of the ligand-bound and ligand-free GroEL species.

DISCUSSION

In this report we investigated the effect of high hydrostatic pressure on the dissociation of the GroEL 14mer. In the course of this study we have detected heterogeneity present in the preparation of this oligomeric protein. In an earlier study we had observed that the dissociation of GroEL at 1−3 kbar pressure was controlled by both thermodynamics and kinetics (*19*). The kinetics at fixed pressures led to the dissociation of the oligomer into monomers only to a certain extent and thus indicated apparent plateaus at various pressures. This result was confirmed by the analysis of the products by native gel electrophoresis (*19*). Such observations are usually referred to as indications of deterministic equilibria and have been observed in the dissociation of many dimeric, trimeric, and oligomeric proteins (see the introduction). Deterministic behavior arises when the classical thermodynamic equilibrium, expected to result from a large number of stochastic events, is not established (*1*, *2*, *44*). Weber (*1*) pointed out that the deterministic character of molecular processes observed on a macroscopic scale could be attributed to the results from the statistics of a number of independent stochastic events. Some of the important characteristics of systems showing deterministic behavior are slow reassociation rates, independence of dissociation rates on concentration, and apparent heterogeneity in species, with each component behaving in a stochastic manner in a process such as dissociation (see the introduction). The presence of heterogeneity in the GroEL species cannot be easily assessed by common techniques such as sedimentation velocity, HPLC, gel electrophoresis, or dissociation by chaotropes. Heterogeneity could also result from the binding of ligands such as KCl or Mg^{2+} that are added during the purification. Since the molecular weights of these ligands are insignificant compared to the mass of the GroEL (840 kDa), the use of mass spectroscopy is also not suitable to distinguish the heterogeneous species. Therefore, the investigation of the phenomenon by comparing the high-pressure dissociation kinetics under various conditions is a very plausible method. A single preparation of GroEL was used throughout the investigation to avoid inconsistencies.

In an earlier investigation we have reported that upon depressurization there was no apparent reassociation of the monomers to produce 14mers (*19*). Although from the fluorescence increase after depressurization of GroEL samples the reassociation rate kinetics was shown to have a $t_{1/2}$ of 150 h at 25 °C (*22*), in the present study we were unable to detect any significant increase in light scattering intensity after the depressurization. Incomplete dissociation with no apparent reassociation on depressurization means that the reassociation rate is much less than the dissociation rate, so if the equilibrium was stochastic, all of the GroEL should dissociate. In this investigation, the lack of reversibility in the dissociation process is different from the cases where deterministic equilibria were observed (*25*, *27*, *32*). In those cases, subunit dissociation was fully reversible upon depressurization. In the pressure-induced dissociation of a tetrameric protein, yeast glyceraldehyde-3-phosphate dehydrogenase, Cioni and Strambini have addressed the pitfalls connected with the use of deterministic equilibrium in pressure dissociation studies (*32*). The observation that the observed dissociation rates are independent of the GroEL concentration is evident from Figure 3. Under identical reaction conditions, the slope of the line in a plot of $k_{1,obs}$ (the major phase of the reaction) vs [GroEL] is very small and, in fact, showed a negative value. This is not unexpected in our study, since any reassociation of GroEL monomers is extremely slow. However, the situation is completely different from the studies where a persistent (long-lived) conformational heterogeneity is generated in the protein ensemble and shows a lack of protein concentration dependence of subunit association (*5*, *25*, *44*). Therefore, the dissociation of the GroEL 14mer by high hydrostatic pressure discussed in this investigation most probably follows a "deterministic behavior" but not deterministic equlibria. Therefore, conformational species leading to pressure-dependent kinetics are due to the

presence of hetergeneous conformations already present in the native GroEL-14 mer, rather than arising from extremely slow equilibria established during the dissociation process.

The next important aim was to determine the effect of KCl and/or Mg^{2+} binding on GroEL heterogeneity. At 2.5 kbar, both of the observed rates ($k_{1,obs}$ and $k_{2,obs}$ obtained from biexponential fits) decreased exponentially with the increase in [KCl] and reached a minimum at ~75 mM (Figure 4). Similarly, the observed fast ($k_{1,obs}$) and slow ($k_{2,obs}$) rates decreased with the increase in [Mg^{2+}] and reached a minimum at ~3 mM Mg^{2+} (Figure 5). These observations indicate that the binding of either KCl or Mg^{2+} imparts some tightness to the GoEL structure, making the dissociation processes slower. Under saturating concentrations of KCl and Mg^{2+}, the magnitude of the observed fast rate ($k_{1,obs}$) is about 4 times slower than in 100 mM KCl and is similar to that with 10 Mg^{2+} alone (see Table 1). The slower rate ($k_{2,obs}$) is about 4.5 times slower than that in 100 mM KCl but is 2 times faster than in 10 mM Mg^{2+} (Table 1). These differences cannot be explained easily, but we speculate that it is a matter of introducing heterogeneity when the two ligands are added together. It is interesting to note that the slow phases of the reactions in the presence of Mg^{2+}, KCl, and Mg^{2+} + KCl have the maximum amplitudes whereas in the fast phase in buffer alone dissociation has the maximum amplitude (91% total). This observation appears as a change in the dissociation mechanism at this constant pressure of 2.5 kbar, most probably due to the change in the ratios of the ligand-bound and ligand-free GroEL species.

In conclusion, results from this study, in the absence of any denaturant, are important for detecting and understanding heterogeneity in GroEL preparations associated with the different amount of ligands bound to the oligomer.

REFERENCES

1. Weber, G. (1992) *Protein Interactions*, Chapman and Hall Inc., New York.
2. Weber, G. (1993) *J. Phy. Chem. 97*, 7108−7115.
3. Silva, J. L., and Weber, G. (1993) *Annu. Rev. Phys. Chem. 44*, 89−113.
4. Mozhaev, V. V., Heremans, K., Frank, J., Masson, P., and Balny, C. (1996) *Proteins 24*, 81−91.
5. Rietveld, A. W., and Ferreira, S. T. (1996) *Biochemistry 35*, 7743−7751.
6. Cioni, P., and Strambini, G. B. (1996) *J. Mol. Biol. 263*, 789−799.
7. Drljaca, A., Hubbard, C. D., van Eldik, R., Asano, T., Basilevsky, M. V., and Le Noble, W. J. (1998) *Chem. Rev. 98*, 2167−2289.
8. Lassalle, M. W., Yamada, H., and Akasaka, K. (2000) *J. Mol. Biol. 298*, 293−302.
9. Galan, A., Sot, B., Llorca, O., Carrascosa, J. L., Valpuesta, J. M., and Muga, A. (2001) *J. Biol. Chem. 276*, 957−964.
10. Seemann, H., Winter, R., and Royer, C. A. (2001) *J. Mol. Biol. 307*, 1091−1102.
11. Webb, J. N., Webb, S. D., Cleland, J. L., Carpenter, J. F., and Randolph, T. W. (2001) *Proc. Natl. Acad. Sci. U.S.A. 98*, 7259−7264.
12. Silva, J. L., Foguel, D., and Royer, C. A. (2001) *Trends Biochem. Sci. 26*, 612−618.
13. Sherman, W. F., and Stadtmuller, A. A. (1987) *Experimental Techniques in High-Pressure Research*, Wiley, Chichester.
14. Jannasch, H. W., Marquis, R. E., and Zimmerman, A. M. (1987) in *Current Perspectives in High-Pressure Biology*, Academic Press, Orlando, FL.
15. van Eldik, R., and Jonas, J. (1987) in *NATO ASI Series (Adv. Sci. Inst.) Ser. C: Math. Phys. Sci. 197*, Reidel, Dordrecht, The Netherlands.
16. Winter, R., and Jonas, J. (1993) in *NATO ASI Series (Adv. Sci. Inst.) Ser. C: Math. Phys. Sci. 401*, Kluwer Academic Publishers, Dordrecht, The Netherlands.
17. Markley, J. L., Northrop, D. B., and Royer, C. (1996) *High-Pressure Effects in Molecular Biophysics and Enzymology*, Oxford University Press, New York.
18. Holzapfel, W. B., and Isaacs, N. (1997) *High-Pressure Techniques in Chemistry and Physics*, Oxford, Oxford.
19. Panda, M., Ybarra, J., and Horowitz, P. M. (2001) *J. Biol. Chem. 276*, 6253−6259.
20. Paladini, A. A., Jr., and Weber, G. (1981) *Biochemistry 20*, 2587−2593.
21. Gross, M., and Jaenicke, R. (1994) *Eur. J. Biochem. 221*, 617−630.
22. Gorovits, B. M., Raman, C. S., and Horowitz, P. M. (1995) *J. Biol. Chem. 270*, 2061−2066.
23. Silva, J. L., Miles, E. W., and Weber, G. (1986) *Biochemistry 25*, 5780−5786.
24. Ruan, K., and Weber, G. (1988) *Biochemistry 27*, 3295−3301.
25. Erijman, L., and Weber, G. (1991) *Biochemistry 30*, 1595−1599.
26. Erijman, L., Lorimer, G. H., and Weber, G. (1993) *Biochemistry 32*, 5187−5195.
27. Rietveld, A. W., and Ferreira, S. T. (1998) *Biochemistry 37*, 933−937.
28. Pedrosa, C., and Ferreira, S. T. (1994) *Biochemistry 33*, 4046−4055.
29. King, L., and Weber, G. (1986) *Biochemistry 25*, 3632−3637.
30. Royer, C. A., Weber, G., Daly, T. J., and Matthews, K. S. (1986) *Biochemistry 25*, 8308−8315.
31. Ruan, K., and Weber, G. (1989) *Biochemistry 28*, 2144−2153.
32. Cioni, P., and Strambini, G. B. (1997) *Biochemistry 36*, 8586−8593.
33. Silva, J. L., and Weber, G. (1988) *J. Mol. Biol. 199*, 149−159.
34. Dreyfus, G., Guimaraes-Motta, H., and Silva, J. L. (1988) *Biochemistry 27*, 6704−6710.
35. Silva, J. L., Silveira, C. F., Correia Junior, A., and Pontes, L. (1992) *J. Mol. Biol. 223*, 545−555.
36. Sundaram, S., Roth, C. M., and Yarmush, M. L. (1998) *Biotechnol. Prog. 14*, 773−781.
37. Pontes, L., Cordeiro, Y., Giongo, V., Villas-Boas, M., Barreto, A., Araujo, J. R., and Silva, J. L. (2001) *J. Mol. Biol. 307*, 1171−1179.
38. Rholam, M., and Nicolas, P. (1981) *Biochemistry 20*, 5837−5843.
39. Scarlata, S. F., and Royer, C. A. (1986) *Biochemistry 25*, 4925−4929.
40. Xu, G., and Weber, G. (1982) *Proc. Natl. Acad. Sci. U.S.A. 79*, 5268−5271.
41. Weber, G. (1986) *Biochemistry 25*, 3626−3631.
42. Silva, J. L., Villas-Boas, M., Bonafe, C. F., and Meirelles, N. C. (1989) *J. Biol. Chem. 264*, 15863−15868.
43. Gomes, F. C., Pereira, E. R., Bonafe, C. F. S., and Silva, J. L. (1990) (Preaux, G., and Leontie, L., Eds.) pp 315−318, Leuven University Press, Leuven, Belgium.
44. Ferreira, S. T., and De Felice, F. G. (2001) *FEBS Lett. 498*, 129−134.
45. Horwich, A. L., Low, K. B., Fenton, W. A., Hirshfield, I. N., and Furtak, K. (1993) *Cell 74*, 909−917.
46. Fayet, O., Ziegelhoffer, T., and Georgopoulos, C. (1989) *J. Bacteriol. 171*, 1379−1385.
47. Cheng, M. Y., Hartl, F. U., Martin, J., Pollock, R. A., Kalousek, F., Neupert, W., Hallberg, E. M., Hallberg, R. L., and Horwich, A. L. (1989) *Nature 337*, 620−625.
48. Braig, K., Otwinowski, Z., Hegde, R., Boisvert, D. C., Joachimiak, A., Horwich, A. L., and Sigler, P. B. (1994) *Nature 371*, 578−586.
49. Braig, K., Adams, P. D., and Brunger, A. T. (1995) *Nat. Struct. Biol. 2*, 1083−1094.

50. Boisvert, D. C., Wang, J., Otwinowski, Z., Horwich, A. L., and Sigler, P. B. (1996) *Nat. Struct. Biol. 3*, 170−177.
51. Xu, Z., Horwich, A. L., and Sigler, P. B. (1997) *Nature 388*, 741−750.
52. Lorimer, G. (1997) *Nature 388*, 720−721, 723.
53. Xu, Z., and Sigler, P. B. (1998) *J. Struct. Biol. 124*, 129−141.
54. Thirumalai, D., and Lorimer, G. H. (2001) *Annu. Rev. Biophys. Biomol. Struct. 30*, 245−269.
55. Buchner, J., Schmidt, M., Fuchs, M., Jaenicke, R., Rudolph, R., Schmid, F. X., and Kiefhaber, T. (1991) *Biochemistry 30*, 1586−1591.
56. Goloubinoff, P., Christeller, J. T., Gatenby, A. A., and Lorimer, G. H. (1989) *Nature 342*, 884−889.
57. Laminet, A. A., Ziegelhoffer, T., Georgopoulos, C., and Pluckthun, A. (1990) *EMBO J. 9*, 2315−2319.
58. Martin, J., Langer, T., Boteva, R., Schramel, A., Horwich, A. L., and Hartl, F. U. (1991) *Nature 352*, 36−42.
59. Viitanen, P. V., Lubben, T. H., Reed, J., Goloubinoff, P., O'Keefe, D. P., and Lorimer, G. H. (1990) *Biochemistry 29*, 5665−5671.
60. Todd, M. J., Viitanen, P. V., and Lorimer, G. H. (1994) *Science 265*, 659−666.
61. Yifrach, O., and Horovitz, A. (2000) *Proc. Natl. Acad. Sci. U.S.A. 97*, 1521−1524.
62. Horovitz, A., Bochkareva, E. S., Kovalenko, O., and Girshovich, A. S. (1993) *J. Mol. Biol. 231*, 58−64.
63. Bonafe, C. F., Villas-Boas, M., Suarez, M. C., and Silva, J. L. (1991) *J. Biol. Chem. 266*, 13210−13216.
64. Bonafe, C. F., Araujo, J. R., and Silva, J. L. (1994) *Biochemistry 33*, 2651−2660.
65. Gorovits, B., Raman, C. S., and Horowitz, P. M. (1995) *J. Biol. Chem. 270*, 2061−2066.
66. Vinckier, A., Gervasoni, P., Zaugg, F., Ziegler, U., Lindner, P., Groscurth, P., Pluckthun, A., and Semenza, G. (1998) *Biophys. J. 74*, 3256−3263.
67. Staniforth, R. A., Cortes, A., Burston, S. G., Atkinson, T., Holbrook, J. J., and Clarke, A. R. (1994) *FEBS Lett. 344*, 129−135.
68. Jai, E. A., and Horowitz, P. M. (1999) *J. Protein Chem. 18*, 387−396.
69. Clark, A. C., Hugo, E., and Frieden, C. (1996) *Biochemistry 35*, 5893−5901.
70. Neuman, R. C., Jr., Kauzman, W., and Zipp, A. (1973) *J. Phys. Chem. 77*, 2687.
71. Weber, G., and Daniel, E. (1966) *Biochemistry 5*, 1900−1907.
72. Weber, G., and Anderson, S. R. (1969) *Biochemistry 8*, 361−371.
73. Rye, H. S., Burston, S. G., Fenton, W. A., Beechem, J. M., Xu, Z., Sigler, P. B., and Horwich, A. L. (1997) *Nature 388*, 792−798.

BI011794C